Water flows through mussel rafts and their relationship with wind speed in a coastal embayment (Ría de Ares-Betanzos, NW Spain)

S. Piedracoba[1*], X.A. Álvarez-Salgado[2], U. Labarta[2], M.J. Fernández-Reiriz[2], B. Gómez[3], C. Balseiro[3]

[1] Universidad de Vigo, Departamento de Física Aplicada, Campus Lagoas-Marcosende, 36310 Vigo, Spain

[2] CSIC Instituto de Investigaciones Marinas, Eduardo Cabello 6, 36208 Vigo, Spain

[3]MeteoGalicia - Consellería de Medio Ambiente, Territorio e Infraestruturas - Xunta de Galicia, Roma 6. 15707 Santiago de Compostela, Spain

Date: 2 December 2013

Abstract

Knowledge of water flows through mussel rafts and their controlling factors is required for an ecosystem approach to the sustainable management of this culture in the Galician rías. With this aim, 4 acoustic 2D-ACM current meters were hung from the bow of 4 rafts located in the mussel cultivation areas of the Ría de Ares-Betanzos (NW Spain) during autumn 2007. Simultaneously, an Aanderaa DCM12 Doppler profiler was moored in an area free of rafts in the middle ría. There were differences in the subtidal and tidal dynamics of the middle channel and mussel farm areas. The tide explained 51.5% of the total variance of the surface current in the middle ría. The explained variance in the seed collection areas of Redes (inner ría) and Miranda (outer ría), where only 2–3 rafts are anchored, were 64.1% and 16.8%, respectively. In the cultivation areas of Arnela (inner ría) and Lorbé (middle ría), where 101 and 40 rafts are anchored, 14.3% and 53.4% of the total variance was explained by the tide. These disparities in the contribution of the tide are likely due to a combination of topographic and bathymetric differences among sites and distortions of the natural flow by the rafts and their hanging ropes. Furthermore, there was a marked influence of winds on the subtidal currents within the rafts; contrasting correlation coefficients and lag times between wind speed and currents were observed for the outer and inner sides of the embayment. The filtration rate of the growing mussels and the number of mussels per raft allow an efficient clearing of the particles transported across the hanging ropes by the measured subtidal currents of 2–3 cm s^{-1} characteristic of the cultivation areas of Arnela and Lorbé.

KEY WORDS: subtidal currents, tidal currents, coastal winds, mussel rafts, ría

1. Introduction

Scientific knowledge of the meteorology, physical oceanography, and biogeochemistry of marine ecosystems is compulsory for an ecosystem-based sustainable management of marine living resources (Dempster and Sanchez-Jerez, 2008; Cranford, et al., 2012). In the particular case of the cultivation of the blue mussel *Mytilus galloprovincialis* on hanging ropes in the coastal embayments of NW Spain, this information is crucial to manage larvae settlement and recruitment strategies (Peteiro et al., 2011), mussel growth rates and carrying capacities (Pérez-Camacho et al., 1995; Peteiro et al., 2006; Babarro et al., 2000; Duarte et al 2008), mussel rafts closures due to the recurrent occurrence of harmful algal blooms (Alvarez-Salgado et al., 2008; 2011; Pérez et al., 2010) and the potential environmental risks of mussel raft culture (Tenore et al., 1982; Alonso-Pérez et al., 2010).

The NW coast of Spain is at the northern boundary of the large marine ecosystem embraced by the Iberian-Canary eastern boundary upwelling system (Arístegui et al. 2009). In this area, upwelling-favourable northerly winds prevail from March-April to September-October in response to the seasonal migration of the Azores High. Downwelling-favourable southerly winds are dominant the rest of the year (Wooster et al., 1976; Bakun and Nelson, 1991; Arístegui et al., 2009). Upwelling events occur with a periodicity of 10–20 days during the upwelling season (Blanton et al., 1987; Álvarez-Salgado et al., 1993), hence modulating the entry and allowing the efficient consumption of new nutrients within the eighteen coastal embayments, collectively known as "rías", which occupy this intricate coastline (Pérez et al., 2000; Villegas-Ríos et al., 2011).

The rías are unique systems because of their morphology and orientation that, together with the freshwater inputs, strongly influence the fate of the upwelled nutrients and the resulting biogenic materials (Blanton et al., 1987; Arístegui et al., 2009; Álvarez-Salgado et al., 2010). The Rías Baixas, located to the south of Cape Fisterra (Figure 1), are oriented in the NE-SW direction, which favours the inflow of upwelled Eastern North Atlantic Central Water (ENACW) in response to northerly winds and are large enough (2.5–4.3 km^3) to efficiently consume the upwelled nutrients leading to average daily primary production rates as high as 3 g C m^{-2} d^{-1} during the upwelling season (Arístegui et al., 2009). Continental runoff gains importance during the downwelling season, contributing significantly to the dynamics and biogeochemistry of these embayments (Nogueira et al., 1997; Álvarez-Salgado et al., 2000; 2010). The Rías Altas, located to the north of Cape Fisterra, display a wide variety of sizes, from 0.01 to 0.75 km^3, and coastline orientations, and they receive proportionally larger freshwater inputs than the Rías Baixas (Álvarez-Salgado et al., 2010; 2011; Villegas-Rios et al., 2011). The Rías Altas, specifically the Ría de Ares-Betanzos (Figure 1), also support a significant number of mussel rafts and local fisheries, although their total yield is lower than that of the Rías Baixas (Bode and Varela, 1998).

The hydrodynamics of coastal waters, especially in semi-enclosed bays, together with the nutrient and plankton loads transported by the dominant currents, are the major factors determining the balance between suspended particles depletion and renewal in marine farms. In fact, the ingestion capacity is a function of phytoplankton concentration and current speed (Frechette et al., 1989). Furthermore, marine farm structures cause drag reducing water flows within farmed areas (Plew et al., 2005; Strohmeier et al., 2005; Fan et al., 2009). It has

also been shown that shellfish farms induce changes in the estuarine circulation patterns, with important implications for local food depletion (Duarte et al., 2008; Plew et al., 2011). Consequently, it is important that the effects of farm structures are considered when estimating water flows within a cultivation area. In our particular case, by measuring the current velocity within a mussel raft, the drag effects of both the raft where the current meter is hung and the surrounding structures are implicitly included. Therefore, our measurements would reflect the currents as experienced by the mussels in the hanging ropes. This information will allow calculating the real fluxes experienced by mussels and are also suitable to validate numerical models that predict intra-rafts currents.

There are only two studies of currents through rafts based on empirical data (Blanco et al., 1996; Boyd and Heasman, 1998) and another one based on a numerical model (Grant and Bacher, 2001). Other studies emphasize how the number of ropes per raft in a mussel farm together with the thousands of mussels on each rope can modify the local flow (Plew, 2011; Stevens et al., 2008; Strohmeier et al., 2005) and, consequently, the food availability.

As a first step to monitor the matter and energy flow through the mussel raft cultivation areas of the Ría de Ares-Betanzos, current meters were simultaneously hung in four mussel rafts located in two areas where the mussels are cultured, Arnela and Lorbé, and two areas of mussel seed capture, Redes and Miranda (Figure 1). In addition, a Doppler profiler was moored in an area free of rafts in the middle channel of the ría (DCM12, Figure 1) over the same period. We measured the water flow through these singular cultivation platforms in order to study the spatial similarities and differences at tidal and subtidal scales between the currents measured at the four cultivation areas and the middle channel of the

ría in relation with: 1) natural spatial differences related with both steady (topography, bathymetry) and transient (continental runoff, remote and local winds) main forcing agents; and 2) man-made differences derived from the distortion of the natural flow due to the dense array of mussel rafts in the cultivation areas (see inset of Figure 1). However, freshwater discharges were so low and invariable (CV ~ 2%) during the study period (data not shown) that this forcing had to be excluded from the analysis.

We should emphasize that our measurements are indicative of velocities within the rafts, which are more relevant to mussel culture than velocities measured nearby the rafts, because they are the velocities experienced by the hanging mussels. Soundly, water flows based on within-raft velocities can be coherently compared with the water flows filtered by the mussel hung on the rafts. In practice, it is not possible to measure currents unaffected by the rafts at the same sites where the mussel farms are located. Therefore, separation of the effect of the rafts from the effect of the location (topography and bathymetry) is not feasible. However, the results of this work will help to understand the differences in the productivity of the mussel cultivation and seed caption areas, providing scientifically-based advice to mussel farmers.

2. Materials and methods

2.1. Study site

The Ría de Ares-Betanzos is a V-shaped coastal inlet located in the Galician coast (NW Spain) between Cape Fisterra and Cape Prior, freely connected with the adjacent shelf (Figure 1). It consists of two branches: Ares, the estuary of river Eume, and Betanzos, the estuary of river Mandeo, with long-term average flows

of 16.5 m^3 s^{-1} and 14.1 m^3 s^{-1}, respectively (Prego et al. 1999, Sanchez-Mata et al. 1999). The two branches converge into a confluence zone that opens to the adjacent shelf through a mouth that is 40 m deep and 4 km wide. From the hydrographic point of view, the two branches can be considered as partially mixed estuaries where fresh and marine waters mix gradually (Sánchez-Mata et al., 1999; Gómez-Gesteira and Dauvin, 2005). By contrast, the confluence and outer zones can be considered as an extension of the adjacent shelf that it is affected by the intensity, persistence, and direction of coastal winds (Bode and Varela, 1998; Villegas-Ríos et al. 2011).

The Ría de Ares-Betanzos supports 147 rafts that produce about 10,000 metric tons of the blue mussel *Mytitlus galloprovinciallis* per year (Labarta et al., 2004). Reproductive adults are concentrated in the southern shore of the ría, in Arnela (40 rafts) and Lorbé (101 rafts, Figure 1). Therefore, blue mussels of the Ría de Ares-Betanzos must be considered as a meta-population whose dynamics has been altered by extensive cultivation activities (Peteiro et al. 2011). Since the parental stock is maintained from year to year to guarantee a minimum commercial production, mussel abundance on the rafts does not depend on settlement success. Therefore, spatial differences in larval supply and settlement magnitude will be more affected by the local circulation patterns than by the adult population structure (Ladah et al., 2005; Peteiro et al., 2011).

The mussel rafts are made from eucalyptus trusses that are attached to floats and anchored by one point to concrete blocks on the sea bed. Each raft has a maximum surface area 20 m x 25 m (= 500 m^2) and contains up to 500 ropes with a range of length from 6 to 12 m (Labarta et al., 2004). The distance between neighbouring rafts within a cultivation polygon is around 100 m.

2.2. Current measurements

Four acoustic FSI 2D-ACM current meters were hung simultaneously at 1 m depth at the bow of four mussel rafts located in the northern (Miranda and Redes) and the southern (Lorbé and Arnela) side of the Ría de Ares-Betanzos (Figure 1). They were deployed from 15 October to 20 November 2007 recording data at 5 minute intervals.

An Aanderaa DCM12 acoustic Doppler current profiler (ADCP) was moored in the middle ría at 20 m depth (Figure 1). The DCM12 was installed in a gymbal system at the top of a pyramidal structure. This mooring also covered the period from 15 October to 20 November 2007. The DCM12 measures the current velocity at 5 depth intervals using the Doppler effect with a transmitted signal of 606.7 kHz. From the surface to 4 m above the instrument, the DCM12 divides the water column into five partially overlapped layers and records the depth integrated velocity of each one. With the selected configuration, all layers were 4.5 m in size, and their respective centre depths were approximately at 2.7 (layer D1), 5.3 (D2), 8.0 (D3), 10.7 (D4) and 13.3 m (D5) from the surface. The recording interval of the DCM12 was set to 10 min. Additionally, the DCM12 has a high precision quartz pressure sensor (Quartzonic Pressure Sensor model 960A) which measures the water level.

2.3. Remote and local winds

Remote winds were obtained at 1 hour intervals from the Seawatch buoy of the Spanish Agency Puertos del Estado off Cape Vilano (http://www.puertos.es) and local winds were reconstructed at the three 4 km x 4 km cells shown in Figure 1 by the WRF_ARW model run operationally by the Galician Meteorological Agency Meteogalicia (http://www.meteogalicia.es). The atmospheric modelling

system of Meteogalicia uses Global model GFS as initial and boundary conditions and includes 3 nested domains to forecast the evolution of the atmosphere up to 4 days in advance. Nested domains consist of a 36 km domain that covers South Western Europe, a 12 km resolution domain covering Iberian Peninsula and a 4 km resolution domain covering Galicia Region (used in this study).

2.4. Analysis of the tidal and subtidal components of the currents

We used three techniques to compare the measured currents at each site (Miranda, Redes, Lorbé, Arnela and DCM 12) and wind data: 1) a Fast Fourier Transform (FFT) of the currents to test differences between sites; 2) a least-squares harmonic decomposition to calculate tidal constituents; and 3) a low pass filter applied to the current and wind time-series to remove variability at tidal and higher frequencies in order to study subtidal currents.

The Fast Fourier Transform (FFT) was calculated considering the total vector currents measured at each site. Anti-clockwise and clockwise components of the Fourier transform of current velocities for the four rafts and the middle ría were calculated.

We used T_tide, an open source MATLAB toolbox produced by Pawlowicz et al. (2002), to separate out the tidal from the non-tidal components of the currents by performing a harmonic tidal analysis on the 2D-ACM and DCM12 currents. A set of harmonic tidal analyses was performed on all total vector data points corresponding to the five positions (4 in the rafts and 1 in the middle channel) for 35 days in October-November 2007. A smoothing filter $A2^2A3$ (three consecutively running averages: two of them with a window size of two samples, i.e. 1 h, and one with three samples, i.e. 1-1/2 h) was applied first to the velocity currents data to eliminate high frequency currents and noise (periods less than 1h).

A $A24^2A25$ filter with a cut-off period of 30 h was applied to the time series of currents and wind to remove the variability at tidal or higher frequencies (Godin, 1972). The output of applying the $A2^2A3$ filter to the raw data (high pass filtered currents) was subtracted to the output of applying the $A24^2A25$ filter with a cut-off period of 30 h to the raw data (low pass filtered currents), to obtain a band pass time series with energy between 1 and 30 h . The harmonic tidal analysis was applied to the later time series.

2.5. Cross correlation between winds and subtidal currents

The cross-correlation analysis is a statistical tool that allows calculation of the correlation between two time series, W(t) and V(t + t), that are out of phase with a lag time t. The shape of the cross-correlation coefficient curve R(t) versus t represents the variation of the correlation between the two time series depending on the lag time. This analysis was applied to the low frequency (subtidal) vector currents and the low frequency vector winds recorded off Cape Vilano and simulated by the WRF_ARW model within the ría during the study period. Although the recording interval of the 2D-ACM and DCM12 current meters were set to 5 minute and 10 minute intervals, respectively, ensemble time averaging of the current meters was 1 hour in order to correlate with winds which were obtained at 1 hour intervals.

3. Results

3.1 Tidal range and total currents

The time-series of tidal height during the recording period included two spring tides (on 20 October and 3 November 2007) and two neap tides (on 27 October and 10 November 2007). Spring and neap tidal ranges were between 2.8 m and

3.9 m, and between 0.7 m and 1.7 m, respectively (Figure 2a). A harmonic analysis of the tidal height at the position of the DCM12 revealed that the main harmonics were the semidiurnal M2, S2 and N2, with amplitudes of 1.2 ± 0.1, 0.4 ± 0.1 and 0.3 ± 0.1 m, respectively, and the diurnal harmonics K1 (0.1 ± 0.1 m) and O1 (0.1 ± 0.1 m). Figure 2b-j shows the observed current time series at all the current meter locations. There were differences between the maximum current recorded at each location. Maximum celerities were lower at Arnela (12.3 cm s^{-1}) and Lorbé (15.5 cm s^{-1}), where most of the rafts are located, than at Redes (23.2 cm s^{-1}) and Miranda (27.2 cm s^{-1}). Maximum celerity was the highest in the middle channel, decreasing from surface (37 cm s^{-1} at D1 and D2) to bottom layers (25 cm s^{-1} at D4 and D5).

3.2. Spectral Analysis of the 2D-ACM and DCM12 total currents

The rotary spectral analysis on the 35 days of current meter data showed significant energy differences at all frequencies, especially at semidiurnal and lower frequencies (T > 30 h) between currents measured in the raft polygons (Figure 3) and the middle ría (Figure 4). At the rafts, Arnela showed the lowest energy at all frequencies and Redes was characterized by the highest energy at semidiurnal frequency. The semidiurnal peaks in Lorbé and Miranda were not as well-defined as in Redes. The outer sites, Miranda and Lorbé, displayed higher energy at lower frequencies than the inner sites, Arnela and Redes. There were no significant differences between counter-clockwise (CCW) and clockwise (CW) energy at all rafts. Conversely, the rotary spectral analysis of the surface currents in the middle ría was comparable in magnitude only to the spectra from Redes, but it was significantly different at diurnal and lower frequencies. In fact, the diurnal peak was almost negligible at all rafts. The CCW and CW energy peaks

were very similar at the surface (D1) in the middle ría (Figure 4). Only in the second layer (D2) the CW semidiurnal energy peak is higher than CCW energy peak. The most energetic tidal harmonics were not found in the surface layer (0–4.5 m), as could be expected, but in the second one. This was previously found by Míguez (2003) in the rías of Vigo and Pontevedra and by Piedracoba et al. (2005) in Ribadeo. As mentioned in Piedracoba et al. (2005), whether this is a natural physical process (wind/wave induced turbulence at the surface layer) or an instrumental artefact is not clear yet. Because the DCM12 was designed to reduce the side-lobe effect (Aanderaa et al. 1995, Aanderaa Instruments, 1999), this can cause artificial effects on surface measurements that lead to under estimate of surface velocities (van Haren, 2001). The energy peaks indicates that the energy in the surface layer of the middle ría at the lower (T > 30h) frequencies is higher than the energy at these frequencies at the rafts position.

In the following sections the tidal and subtidal bands will be described focusing on the relationship between subtidal currents and wind forcing. As stated in the introduction, freshwater discharges from rivers Mandeo (1.4 ± 0.3 m^3 s^{-1}) and Eume (4.4 ± 0.1 m^3 s^{-1}) were so low and invariable (CV ~ 2%) during the study period that this forcing was excluded from the analysis because its influence on the variability of the measured currents was negligible.

3.3. Tidal currents

Harmonic tidal analyses were performed on total vector data of the 5 study sites for the 35 days that the instruments were recording in October-November 2007 (Table 1 and 2). Only constituents with significant amplitudes and signal to noise ratios > 2 are listed. Percentages of total variance explained by the tide at the raft positions were 64.1%, 53.4%, 16.8% and 14.3% for Redes, Lorbé, Arnela and

Miranda, respectively. Major axis of the most important constituent, M2, was also very different at the four raft sites: 4.2 ± 0.5, 1.7 ± 0.2 and 1.0 ± 0.7 cm s^{-1} for Redes, Lorbé and Arnela and it was absent in Miranda. Therefore, there was a positive relationship between the percentage of total variance explained by the tide and the tidal velocity explained by the harmonic M2. Redes and Lorbé were the positions where the signal-to-noise ratios were higher for the most important harmonics (M2, N2 and S2) for this 35 days period. Tidal currents were rectilinear (no preferred sense of rotation) in Miranda and Lorbé (eccentricity close to 1) and tended to accommodate to the shape of the ría with a mean along-channel orientation for the most important harmonic constituents (M2 inclination was 108º ± 77º and 139º ± 8º for Miranda and Lorbé, respectively). However, the inclination of the most relevant semidiurnal constituents in Redes was about 20º ± 20º and, therefore, tidal currents in Redes did not follow the main axis of the ría as in the outer positions.

In the middle ría, the major axis of the K1 constituent at layer D1 was especially high due to the breeze effect as found in other Galician Rías (Míguez, 2003). The maximum tidal speed and semi-major axis of the most important semidiurnal component (M2) was found at D2 (3.1–7.5 m) as also recorded in other Galician Rías (Míguez, 2003, Piedracoba et al. 2005). From D2 to D5, the M2 semimajor axis decreased from 10.7 ± 0.8 to 6.8 ± 0.4 cm s^{-1}. In addition, the M4 and M6 tidal components due to the non-linear momentum advection terms and quadratic bottom friction were amplified from D2 to D5. However, these later components with signal-to-noise ratio > 2 appeared only at the surface in Lorbé. The percentage of total variance explained by the tide increased noticeably from the surface (51.5%) to the subsurface layers (> 86%), although it reduced with depth

from 91.1% at D2 to 86% at D5.

3.4. Subtidal wind forcing

Remote winds at the Vilano buoy and local winds simulated by the WRF_ARW model were low-pass filtered to remove the variability impose by tidal and diurnal cycles and higher frequencies. After this filter, only the variability with periods longer than 30 hours was retained in the subtidal records presented in Figure 5a.

Average and standard deviations of the East and North low-pass filtered wind velocity components, $\overline{W_x} \pm SD_{W_x}$ and $W_y \pm SD_{W_y}$ were –4.7 ± 4.2 and –1.5 ± 2.2 m s^{-1}, respectively. Local winds reconstructed at the three positions of Figure 1 by the WRF_ARW model run operationally were highly correlated with the winds recorded at the Vilano buoy. The correlations were 0.84, 0.80 and 0.72 for Met 1, Met 2 and Met 3, respectively (Figure 1). In fact, the difference between local and remote winds is just a reduction of wind intensity inside the ría. Therefore, it is not possible to discern the relative influence of remote and local winds on the dynamics of the ría. For this reason, although we have used the winds recorded at the Vilano buoy to run the cross correlation analysis with the surface currents, we will not specify whether it is remote or local from here on.

3.5. Subtidal currents

Current velocity data from Arnela, Lorbé, Miranda, Redes and the middle ría were also low-pass filtered to retain only the variability with periods longer than 30 hours in the subtidal records presented in Figure 5 (b-j).

Average and standard deviations of the East and North subtidal current velocity components ($\bar{u} \pm SD_U, \bar{v} \pm SD_V$) were calculated for the surface layers of Arnela (1.0 ± 1.7, –1.4 ± 0.7 cm s^{-1}), Lorbé (–1.9 ± 0.8, 0.2 ± 1.2 cm s^{-1}), Miranda (–5.1

± 0.9, 2.0 ± 1.1 cm s^{-1}), Redes (0.0 ± 0.6, 0.5 ± 1.2 cm s^{-1}) and DCM12 (–7 ± 1.3, 3.2 ± 2.5 cm s^{-1}) during the study period. Significant differences ($p < 0.05$) between all velocity pairs at 1 m depth were found except for the pair vRedes-vLorbé.

The largest subtidal currents were recorded at Miranda and in the middle ría, while the lowest currents were recorded at Redes. The differences in the average current direction at each position were particularly interesting. In the outer and middle sites (Miranda, Lorbé and Central D1) subtidal currents were northwestwards most of the time, while in Arnela they were mainly southeastwards and Redes showed a northwards dominant direction.

3.6. Subtidal currents and wind forcing relationship

The most recurrent wind direction at the Vilano buoy during the study period was around 65º, which promoted a surface outflow in the middle (Lorbé and Central D1) and outer (Miranda) ría. A succession of wind stress-relaxation events were recorded with a periodicity of less than a week (Figure 5a). The study period started with 2 days (16–17 October) of southwesterly winds. Lorbé, Miranda and the middle ría did not respond to this wind, although an outgoing flow was recorded at the three sites, but of different magnitude (Figure 5c, d, f, Figure 6). Arnela responded with a southwestward current and in Redes the current was negligible. From 18 to 21 October there was a wind relaxation period which did not affect the previous circulation pattern at the five study sites. The period between 22 and 24 October was characterized by southwesterly winds. Surface current in Arnela continued being southwestwards and there was marked outgoing flow in the middle ría and Lorbé (Figure 5c, 5f, Figure 6). Surface current was also outgoing in Miranda, but very slow. From 24 October to 11 November there

was an alternation between northeasterly winds and relaxations with a periodicity of about 5 days. Under these conditions, surface currents at Miranda increased and were northwestwards most of the time. However, there was a marked decrease of the flow in Lorbé from 25 October onwards, which denotes that Lorbé and Miranda have not always the same behaviour. Currents in Redes did not seem to respond to changes in the wind regime. In fact, there was an increase in the current at this site from 8 to 16 November that did not correspond to any change in direction or intensity of the winds. From 14 to 19 November, winds relaxed (Figure 5a) and surface currents in Lorbé, Miranda and the middle ría responded with a dramatic reduction of celerity (Figure 5c, d and f). However, surface currents in Arnela increased slightly and continued being southeastwards or southwestwards and currents in Redes conserved a northeastward direction from 16 November onwards (Figure 4e).

A 2-layer circulation pattern, characteristic of partially mixed estuaries, was found from 15 October to 20 November in the middle ría (Figures 5 f-j). The circulation was always positive, i.e. surface outgoing and subsurface incoming, independently of the wind direction but with different speed depending on the winds intensity. It is worth mentioning that on 21–22 October, when winds blew from the southwest (Figure 5a), the whole water column in the middle ría flowed outwards. It indicates that the subsurface layer of the middle ría reversed their flow in response to this change of winds, although the surface flow in the middle ría, Lorbé and Miranda continued to be outwards (Figure 5c, d, and f, Figure 6).

Progressive vector diagrams (PVD) showing the virtual displacement of a water parcel forced by the low-pass filtered currents recorded by a moored current meter were devised for the surface layer of the five study sites from 15 October to 20

November 2007 (Figure 6). Note that PVDs in Figure 6 have been scaled x10 to facilitate the visualization of the trajectories. PVDs show that there were marked differences between the outer (Miranda, Lorbé, and middle ría) and inner (Arnela, Redes) sites and there are also differences in the trajectories between the northern (Miranda, Redes and middle ría) and southern (Lorbé, Arnela) sides of the ría. Surface currents in Lorbé, Miranda and the middle ría were outgoing throughout all the study period independently of the direction of the winds. Differences were found in current speed and, therefore, in total virtual displacements, especially between the northern (Miranda and middle ría) and southern (Lorbé) sides of the ría.

3.6.1 Complex cross-correlation

A complex cross-correlation analysis between the surface current in the middle ría and the four sites in the raft polygons was performed to study the correlation between these five pairs of vector time series as a function of the lag time between currents (Figure 7). Note that the correlation coefficients between pairs of series were always positive, indicating simultaneous increase or decrease of the current module at both sites. The maximum correlation was observed between the middle ría and Miranda with a lag time of less than 12 hour. Next, with Lorbé, with correlation coefficients between 0.8 and 0.9 for lag times of 0 and 96 hour, respectively. The correlation coefficient with Arnela ranged from 0.73 to 0.83 for 0 and 48 hour lag time, respectively. All these correlations were significant at $p < 0.05$ level. Finally, the correlation between the record in the middle ría and Redes was not significant. Concerning the phase, it was positive between the middle ría and Arnela, Lorbé and Miranda indicating a positive (anticlockwise) angle of 152º (i.e., opposite directions) between the middle ría and Arnela, and positive angles

of 18º with Lorbé and 1.2º with Miranda (i.e., similar directions). These results show a similar behaviour of the middle ría with Miranda and Lorbé (high correlation and phase close to 0). The correlation between the middle ría and Arnela was also high, but the phase show opposite displacement and, therefore, the forcing responsible for the circulation in the outer and the inner parts of the ría acts differently. The correlation between the middle ría and Redes was so low ($p >$ 0.10) that the forcing responsible for circulation at both positions have to be different.

A cross-correlation analysis between all possible pairs of currents at the four rafts was also performed (Figure 8). Only the correlations between Arnela and Lorbé, Arnela and Miranda and Lorbé and Miranda were significant at $p < 0.05$ level. The maximum correlation was found between the outer rafts (Lorbé and Miranda). On the other hand, the correlations between Arnela and Redes, Lorbé and Redes and Miranda and Redes are not significant at $p < 0.05$ level. Therefore, there was no relationship between the current pattern in Redes and the other sites. The outer sites (Lorbé and Miranda) were correlated by 0.70 at lag times less than 12 hour and a phase of about 15º. Both Lorbé and Miranda correlated with Arnela with correlation coefficients of 0.90 and 0.65 at lag times of less than 12 hour and phases of 132 º and 155º between Lorbé and Arnela and Miranda and Arnela, respectively.

The cross-correlation analyses between the low-pass filtered winds and the currents measured in the five layers of the middle ría are summarised in Table 3.

The correlation coefficients were calculated for a discrete time. After this, we calculate the average correlation coefficient and phase over 12 hour intervals (0-12, 13-24, 25-36, … 85-96 H). Although all correlations were significant at $p <$

0.05 level, the highest were found at the surface, D1 (0.78 at less than 12 hour lag time) and the two bottom layers (D4, 0.80 at less than 12 hour lag time; and D5 0.86 at 12–24 hour lag time). The lowest correlation was found in D2, which coincided with the level of no motion (LNM) that separates layers that flow in opposite directions. The phase was negative between the wind and D1 showing a clockwise (negative) angle (i.e. the flow was to the right of wind). On the contrary, the phase was positive between the wind and D2 to D5 showing an anticlockwise (positive) angle between winds and subsurface currents. The angle was about 150º between D1 and D5, i.e. both layers flow in opposite directions consistent with the 2-layer circulation pattern characteristic of partially mixed estuaries.

We also studied the cross-correlation between the low-pass filtered winds and the currents measured at the four raft polygons (see Table 4). The maximum correlations were found with Lorbé (0.82 at 49–60 h lag time), Miranda (0.79 at lag times of less than 12 h) and Arnela (0.74 at 37–48 hour lag time). Therefore, Miranda, the most exposed site to coastal winds, responded faster than the other sites. Conversely, there was no relationship between the winds and the northern inner site of Redes at short lag times. Unlike Arnela, Lorbé and Miranda where the correlation decreased with the lag time, the relationship between Redes and the winds increased slightly with the lag time. Again, these results show that there was no relationship between Redes and the other rafts polygons. Interestingly, the phases between Vilano-Lorbé and Vilano-Miranda were negative, i.e. the surface currents at Lorbé and Miranda were rotated to the right of the wind, as occurred in the surface layer of the middle ría. However, the phase between Vilano-Arnela was positive and, therefore, similar to the angle between Vilano and the bottom

layer (D5) of the middle ría.

4. Discussion

Despite the economic importance of mussel cultivation on hanging ropes and the evidence that subtidal circulation patterns can be behind the spatial differences observed in mussel larvae settlement and recruitment (Peteiro et al. 2007, 2011) and mussel growth rates (Pérez-Camacho et al. 1995, Babarro et al. 2000, Peteiro et al. 2006, Duarte et al. 2008), studies of the water flow through mussel rafts are very scarce in the Galician rías (Pérez-Camacho et al. 1995, Blanco et al. 1996). In addition, none of the previous studies have dealt with the relationship between subtidal currents through mussel rafts and the corresponding external physical forcing agents. Knowledge of the spatial and temporal variability of the subtidal circulation in a coastal embayment or estuary is crucial for assessing (i) the potential success of a given location for mussel or other commercial species settlement and growth; and (ii) its carrying capacity. For these reasons, in the present study we have monitored the instantaneous and subtidal currents in 2 locations of the Ría de Ares-Betanzos where mussels are grown (Lorbé and Arnela) and two other locations where mussel seeds are collected on hanging ropes (Miranda and Redes) for a two month period when coastal upwelling was the dominant process. The maximum total current velocity was 10–12 cm s^{-1} higher at Miranda and Redes than at Lorbé and Arnela, where 95% of the rafts of the ría are placed. This difference can be partly due to the larger current drag effect on the sites were most of the rafts are anchored. Such a frictional effect of aquaculture structures was shown before by Grant and Bacher (2011).

The subtidal circulation in the mussel cultivation and seed recruitment areas of the Ría de Ares-Betanzos is affected differently by the wind regime, bathymetry and

topography. Villegas-Ríos et al. (2011) obtained that 80% of the variability of the exchange flux between the confluence and outer zones of this ría (Figure 1) was controlled by coastal winds. Since Miranda and Lorbé are in the middle-outer ría, it is coherent that the variability of the surface subtidal current in the seed collection site of Miranda and the cultivation polygon of Lorbé also depended on coastal winds. Accordingly, Peteiro et al. (2011) have found that mussel recruitment at Miranda depended on the intensity and frequency of coastal winds. Winds from northeast and southwest were the most frequent in the area, causing respective surface currents to southwest and northeast over the shelf and the corresponding perpendicular water transports throughout the Ekman layer (Ekman, 1905). The Ría de Ares-Betanzos is oriented in the NW-SE direction and Miranda is located close to the mouth of its open end. Therefore, upwelling-favourable north-easterly winds should have more influence on Miranda than in the other recruitment and cultivation sites.

The subtidal circulation pattern in Arnela is also related with the wind regime (Table 4). Furthermore, Arnela is sheltered enough to prevent water displacement to the East or Northeast and the lost by advection of nutrients supplied from the adjacent shelf. Arnela follows the premises of several studies that postulate a higher capacity for plankton retention in areas with local topographic characteristics, coastal orientation, and reduced effect of wind on residual circulation that produce relatively larger residence times (Graham and Largier, 1997; Wing et al., 1998; Narváez et al. 2004). Unlike the rest of positions, subtidal currents in Redes are not related with the wind regime (Table 4). However, Redes is the position where the influence of the tide was the highest (the percent of total variance explained by the tide was 64.1%).

Average subtidal current velocities in the mussel cultivation areas of Arnela and Lorbé were around 2–3 cm s^{-1}. These values are much lower than in the main axis of the embayment, where average surface currents of 8 cm s^{-1} were recorded throughout October 2007. This difference is caused by (i) the bathymetry of the ría that enhances bottom friction in the margins compared with the middle of the embayment; (ii) the topography of the ría that protects better the margins than the middle ría from the wind drag; (iii) the friction caused by the hanging ropes of the array of surrounding mussel rafts characteristic of the cultivation polygons; and (iv) the friction caused by the own hanging ropes of a raft (Plew 2011) on which current meters were placed. Three-month average surface current speed recorded by Pérez-Camacho et al. (1995) in three mussel rafts of the nearby Ría de Arousa also ranged from 2 to 3 cm s^{-1}. The magnitude of the average residual currents measured in the middle Ría de Ares-Betanzos and the seed collection area of Miranda, 5 cm s^{-1}, are comparable with the average values recorded in the free water column of other northern and southern Galician rías (Gilcoto et al., 2001; Piedracoba et al., 2005a; 2005b).

Are these relatively low subtidal flows of 2–3 cm s^{-1} compatible with the food demand of the mussels cultured on hanging ropes? Let us consider that (i) there are about 800 mussels per meter of rope; (ii) there are about 500 ropes per raft; (iii) the length of the bow of a mussel raft is 25 m (Labarta et al., 2004); and (iv) each mussel is able to filtrate about 5 litres of seawater per hour (Labarta et al. 1997). It would result that the hanging mussels are able to filter about 556 L s^{-1} per meter depth of raft. Dividing this volume by the width of the bow (25 m) an equivalent filtration speed of 2.2 cm s^{-1} is obtained, which is comparable with the average subtidal velocity recorded in Arnela and Lorbé, where the cultured mussel

stock is located. Therefore, it seems that the filtration speed of the growing mussels coincides with the velocity of the current transporting their food in such a way that they can efficiently clear the water crossing the mussel raft. On this basis, the mussels cultured in Miranda, where the current velocity is about twice than in Arnela and Lorbé, would not be able to clear the water crossing a mussel raft with the same efficiency unless they double either their filtration rate, which is quite unlikely (Filgueira et al., 2008), or the number of ropes per raft increases.

Considering the subtidal flows in relation to filtration rate of mussels it could be argued that if mussels are able to clear all the water moving though a raft this might be detrimental to "downstream" rafts. However, i) the separation between consecutive rafts in a mussel farm is 100 m; ii) the maximum size of a raft is 25 m x 20 m; and iii) the length of the chain did not allow a free displacement of more 10 m in the surface. Therefore, the maximum depletion area of a raft would be about 1000 m^2 (= 35 m x 30 m) whereas the space not available for depletion would be about 9000 m^2 (= 100 m x 100 m – 35 m x 30 m). Consequently, complete depletion at each individual raft should not affect the productivity of the surrounding rafts.

The orientation of the raft relative to the current may cause differences in the effect of the raft on water velocities measured by a current meter moored at the bow of the raft. The spatial variation of the ellipse parameters and the percentage of total variability explained by the tide were different between the northern and southern sides of the ría. While in the northern side of the ría the magnitude of the major axis and the percentage of variance explained by the most important semidiurnal constituents decreased from the inner raft (Redes) to the outer raft (Miranda), in the southern side both parameters increased from the inner (Arnela)

to the outer raft (Lorbé). The percentages of variability explained by the tide cannot be related to the distortion introduced by these platforms because they are not aligned with the currents and, therefore, current meters are not always at the upstream end of the raft. The evidence that the rafts were not aligned with the currents was based on our experience observing the direction of the water flow during the weekly samplings of thermohaline variables on the study rafts in different stages of the tide and additional visits to install and maintain the current meters. A nearby reference with current meters not hung on the rafts would help to study such a distortion. In this sense, it would be very difficult to determine the distance between the current meter hung on the raft and the reference site to ensure that the natural flow were the same at both sites and the reference was far enough from the distortion effects of the array of surrounding rafts. We are conscious that the current meter moored in the middle channel cannot be a reference for the 4 sites where current meters were hung on a raft, because the natural flow without rafts would be different due to the marked bathymetric differences between these sites.

It is likely that this spatial variation is not only related with environmental factors acting differently on these regions and the effect of the surrounding rafts, but also with the fact that the bow of the rafts, where the current meters were hung, is not necessarily oriented to the current. If the raft did not rotate joint with the current, then a decrease of current velocity measured at the bow should occur due to distortion of the flow by the ropes hung in the raft. In the surface layer of the middle ría, where there are not mussel rafts that distort the flow, the tide explained 51.5% of the total variance of the current. This percentage was very similar to Lorbé (53.4%), but far different from Miranda (14.3%) and Arnela (16.8%).

Therefore large disparities in the variability explained by the tide between sites could be due to both changeable orientation, caused by the translation and rotation movements of the rafts, and topography, bathymetry or estuarine circulation. This study cannot separate the effects of the rafts from other effects on the flow.

We propose that the rotation of each individual raft within a polygon could be affected by local winds acting on structures above the water in a different direction to the current, current patterns at the embayment–scale, distortion of the currents by the surrounding rafts at the polygon–scale or vertical variations in current direction and the raft swinging with change in tide. This complex combination of factors seems to provoke that currents do not always enter a raft through the bow. Although the inflow through the raft is probably tidally forced, it should be considered the friction caused by the hanging ropes of the array of surrounding mussel rafts and the friction caused by the own hanging ropes of a raft on which current meters were placed. Therefore, if only one current meter is installed on the raft, it is not possible to discern whether the current recorded is an inflow or an outflow since it is likely that the current do not always enter the rafts through the bow. It should also be considered that the flow is not totally aligned between the upstream and downstream sides of the raft, because the raft itself tend to diverge the flow upstream causing that the flow is not slowed down downstream (Boyd and Heasman, 1998). Blanco et al. (1996) also suggested that there is inflow along the sides of a raft because currents at the rear were higher than in the middle.

Although the direction of the currents can be determined precisely because the 2D-ACM current meters have an internal compass, no compass was installed simultaneously on these rotating platforms to know how the bow is oriented at

each time. For this reason it was not possible to know how the current enters in the raft. In future studies, hanging current meters, should be installed at the four sides and the centre of a raft continuously tracked with a GPS and a compass to record the direction of the water entering and leaving the structure at any side of the raft and any time. With this exhaustive sampling scheme current speed at the raft scale could be evaluated to study the success of the mussel growth from fluxes derived from these velocities.

5. Conclusions

The relatively low residual currents of 2–3 cm s^{-1} recorded in the mussel cultivation areas of the Ría de Ares-Betanzos are compatible with the food demand of the mussels cultured on hanging ropes. In most locations, growing mussels could efficiently clear the water crossing the rafts because filtration speed of the growing mussels is comparable with the velocity of the current transporting their food. However, in Miranda, where the current velocity is double the filtration speed, it would be necessary to increase the number of rafts and/or the number of ropes per raft, which would increase the filtration speed and decrease the current velocity because of the friction caused by the hanging ropes.

During this anomalously dry period, winds played a major role in the subtidal circulation regime of the different cultivation areas of the ría. The orientation of the two inner branches of this embayment, where the growing area of Arnela and the seed collection area of Redes are located, restricts the flushing out induced by the dominant north-easterly winds that blow into the ría and the adjacent shelf. Conversely, the hydrodynamics of the outer ría, where the seed collection area of Miranda and the growing area of Lorbé are located, are more influenced by the

stronger winds that blow over the shelf and the resulting coastal upwelling/downwelling regime.

It is likely that the currents recorded by instruments installed at the bow of the mussel rafts are affected by both the surrounding rafts and the instrumented raft itself. Rafts do not always align with the currents and water may not always enter rafts at the bow. A consequence of this is that the influence of the raft on the current speed recorded at the bow may vary depending on the orientation of the raft to the current. To overcome this difficulty, hanging current meters should be installed at the four sides and the centre of a continuously tracked raft with a GPS and a compass to record the direction of the water flow entering and leaving the raft at each time.

Acknowledgements

We want to express our gratitude to L.G. Peteiro, H. Regueiro and M. García for technical assistance and employees of PROINSA for their help during sampling. We are very grateful to two anonymous reviewers for their helpful comments and suggestions. This study was supported by the contract-project PROINSA Mussel Farm, codes CSIC 20061089 & 0704101100001, and Xunta de Galicia PGIDIT06RMA018E & PGIDIT09MMA038E. Additional support came from the ESSMA project Spain- Canada Grant of MICINN and DFO. S.P. was funded with a CSIC JAE-Doc fellowship to carry out this work. This is a contribution of the Unidad Asociada CSIC-Meteogalicia

References

Aanderaa, I., Iversen, S., Forbord, S., 1995. Acoustic Doppler current meter: shallow water harbor application. Sea Technology 43.

Aanderaa Instruments, 1999. Doppler Current Meter, DCM 12. Reliability and comparison tests, in Sensor & Systems. A newsletter from Aanderaa Instruments, Aanderaa Instruments, 4 pp.

Alonso-Pérez, F., Ysebaert, T., Castro, C.G., 2010. Effects of suspended mussel culture on benthic-pelagic coupling in a coastal upwelling system (Ría de Vigo, NW Iberian Peninsula). J. Exp. Mar. Biol. Ecol. 382, 96–107.

Álvarez-Salgado, X.A., Rosón, G., Pérez, F.F., Pazos, Y., 1993. Hydrographic variability off the Rías Baixas (NW Spain) during the upwelling season. J. Geophys. Res. 98, 14447–14455.

Álvarez-Salgado, X.A., Gago, J., Míguez, B.M., Gilcoto, M., Pérez, F.F., 2000. Surface waters of the NW Iberian Margin: Upwelling on the shelf versus outwelling of upwelled waters from the Rías Baixas. Estuar. Coast. Shelf Sci. 51, 821–837.

Álvarez-Salgado, X.A., Labarta, U., Fernández-Reiriz, M.J., Figueiras, F.G., Rosón, G., Piedracoba, S., Filgueira, R., Cabanas, J.M., 2008. Renewal time and the impact of harmful algal blooms on the extensive mussel raft culture of the Iberian coastal upwelling system (SW Europe). Harmful Algae 7, 849–855.

Álvarez-Salgado, X.A., Borges, A.V., Figueiras, F.G., Chou, L., 2010. Iberian margin: the Rías. In: Liu, K.-K., Atkinson, L., Quiñones, R., Talaue-McManus, L. (Eds.), Carbon and Nutrient Fluxes in Continental Margins: A Global Synthesis. Springer–Verlag, NewYork, ISBN: 978–3–540–92734–1, pp.103–120.

Álvarez-Salgado, X.A., Figueiras, F.G., Fernández-Reiriz, M.J., Labarta, U., Peteiro, L., Piedracoba, S., 2011. Control of lipophilic shellfish poisoning outbreaks by seasonal upwelling and continental runoff. Harmful Algae 10, 121–129.

Arístegui, J., Barton, E.D., Álvarez-Salgado, X.A., Santos, A.M.P., Figueiras, F.G., Kifani, S., Hernández-León, S. , Mason, E., Machu, E., Demarcq, H., 2009. Sub- regional ecosystem variability in the Canary current upwelling. Prog. Oceanogr. 83, 33–48.

Babarro, J.M.F., Fernández-Reiriz, M.J., Labarta, U., 2000. Growth of seed mussel (*Mytilus galloprovincialis* LMK): Effects of environmental parameters and seed origin. J. Shellfish Res. 19, 187–193.

Bakun, A., 1973. Coastal upwelling indices, west coast of North America, 1946–71, NOAA Tech. Rep. NMFS SSRF–671. US: Dep. of Commerce. 103 pp.

Bakun, A., Nelson, C.S., 1991. The seasonal cycle of wind-stress curl in subtropical eastern boundary current regions. J. Geophys. Res. 96 (C12), 1815–1834.

Blanco, J., Zapata, M., Moroño, A., 1996. Some aspects of the water flow through mussel rafts. Sci. Mar. 60, 275–282.

Blanton, J.O., Tenore, K.R., Castillejo, F.F. de, Atkinson, L.P., Schwing, F.B., Lavín, A., 1987. The relationship of upwelling to mussel production in the rías on the Western coast of Spain. J. Mar. Res. 45, 497–511.

Bode, A., Varela, M., 1998. Primary production and phytoplankton in three Galician Rias Altas (NW Spain): seasonal and spatial variability. Sci. Mar. 62, 319–330.

Boyd, A.J., Heasman, K.G., 1998. Shellfish mariculture in the Benguela System: water flow patterns within a mussel farm in Saldanha Bay, South Africa. J. Shellfish Res. 17, 25–32.

Cranford, P.J., Kamermans, P., Krause, G., Mazurié, J., Buck, B.H., Dolmer, P., Fraser, D., Van Nieuwenhove, K., O'Beirn, F.X., Sanchez-Mata, A.,

Thorarinsdóttir, G.G., Strand, Ø, 2012. An ecosystem-based approach and management framework for the integrated evaluation of bivalve aquaculture impacts. Aquacult. Environ. Interact. 2, 193–213.

Dempster, T., Sánchez-Jerez, P., 2008. Aquaculture and Coastal Space management in Europe: An Ecological perspective. In: Aquaculture in the Ecosystem, Holmer, M., et al (Editors), Springer, 326 pp.

Duarte, P., Labarta, U., Fernández-Reiriz, M.J., 2008. Modelling local food depletion effects in mussel rafts of Galician Rias. Aquaculture 274, 300–312.

Ekman, V.W. 1905. On the influence of the earth's rotation o ocean currents, Arkiv Matematik, Astron. Fysik, 2(11), 1–53.

Fan, X., Wei, H., Yuan, Y., Zhao, L., 2009. Vertical structure of tidal current in a typically coastal raft-culture area. Cont. Shelf Res. 29, 2345–2357.

Figueiras, F.G., Labarta, U., Fernández-Reiriz, M.J., 2002. Coastal upwelling, primary production and mussel growth in the Rías Baixas of Galicia. Hydrobiologia 484, 121–131.

Filgueira, R., Labarta, U., Fernández-Reiriz, M.J., 2008. Effect of Condition index on Clearance Rate allometric relationships in mussels. Rev. Biol. Mar. Ocean. 43, 391–398.

Frechette, M., Butman, C.A., Geyer, W.R., 1989. The importance of boundary-layer flows in supplying phytoplankton to the benthic suspension feeder, Mytilus edulis L. Limnology and Oceanogr. 34 (1), 19–36.

Gilcoto, M., Álvarez–Salgado, X.A., Pérez, F.F., 2001. Computing Optimum Estuarine Residual Fluxes with a Multiparameter Inverse Method (OERFIM). Application to the Ría de Vigo (NW Spain). J. Geophys. Res. 106, 31303–31318.

Gómez-Gesteira, J.L., Dauvin, J.C., 2005. Impact of the Aegean Sea oil spill on the subtidal fine sand macrobenthic community of the Ares-Betanzos Ria (North-west Spain). Mar. Environ. Res. 60, 289–316.

Graham, W.M., Largier, J.L., 1997. Upwelling shadows as nearshore retention sites: the example of northern Monterey Bay. Cont. Shelf Res. 17, 509–532.

Grant, J., Bacher, C., 2001. A numerical model of flow modification induced by suspended aquaculture in a Chinese bay. Canadian Journal of Fisheries and Aquatic Sciences 58, 1003–1011.

Hidy, G.M., 1972. A view of recent air–sea interaction research. Bull. Am. Meteorol. Soc. 53, 1083–1102.

Kelly, K.A., Lagerloef, G.S.E., Bernstein, R.L., 1988. Comment on "Empirical orthogonal function analysis of Advanced very High Resolution Radiometer surface temperature patterns in the Santa Barbara channel. J. Geophys. Res. 93 (C12), 15752–15754.

Kundu, P.K., Allen, J.S., 1976. Some three-dimensional characteristics of low frequency current fluctuations near the Oregon coast. J. Phys. Oceanogr. 6, 181–199.

Labarta, L., Fernández-Reiriz, M.J., Babarro, J.M.F., 1997. Differences in physiological energetics between intertidal and raft cultivated mussels (*Mytilus galloprovincialis* Lmk). Mar. Ecol. Progr. Ser. 152, 167–173.

Labarta, U., Fernández-Reiriz, M.J., Pérez-Camacho, A., Pérez-Corbacho, E., 2004. Bateeiros, Mar, Mejillón. Una Perspectiva Bioeconómica (Serie Estudios Sectoriales). Fundación CaixaGalicia, A Coruña, España.

Ladah, L.D., Tapia, F.J., Pineda, J., López, M., 2005. Spatially heterogeneous, synchronous settlement of *Chthamalus* spp. Larvae in northern Baja California. Mar. Ecol. Prog. Ser. 302, 177–185.

Míguez, B.M., 2003. Descripción dinámica de la circulación en dos Rías Baixas: Vigo y Pontevedra. Ph.D. Thesis, Universidade de Vigo, Vigo, Spain, unpublished.

Narváez, D.A., Poulin, E., Leiva, G., Hernández, E., Castilla, J.C., Navarrete, S.E., 2004. Seasonal and spatial variation of nearshore hydrographic conditions in central Chile. Cont. Shelf Res. 24, 279–292.

Nogueira E., Pérez F.F., Ríos A.F., 1997. Seasonal and long–term trends in an estuarine upwelling ecosystem (Ría de Vigo, NW Spain). Estuar. Coast. Shelf Sci. 44, 285–300.

Pawlowicz, R , Beardsley, B, Lentz, S. 2002. Classical tidal harmonic analysis including error estimates in MATLAB using T TIDE. Comp & Geosci. 28, 929–937.

Peteiro, L.G., Babarro, J.M.F., Labarta, U., Fernández-Reiriz, M.J., 2006. Growth of *Mytilus galloprovincialis* after the Prestige oil spill. ICES J. Mar. Sci. 63, 1005–1013.

Peteiro, L.G., Filgueira, R., Labarta, U., Fernández-Reiriz, M.J., 2007. Settlement and recruitment patterns of *Mytilus galloprovincialis* L. in the Ría de Ares-Betanzos (NW Spain) in the years 2004–2005. Aquaculture Res. 38, 957–964.

Peteiro L.G, Labarta, U., Fernández-Reiriz, M.J., Filgueira, R., Álvarez-Salgado, X.A., Piedracoba, S., 2011. Influence of intermittent-upwelling on *Mytilus galloprovincialis* settlement patterns in the Ría de Ares-Betanzos. Mar. Ecol. Prog. Ser., 443, 111–127.

Pérez, F.F., Álvarez–Salgado, X.A., Rosón, G., 2000. Stoichiometry of nutrients (C, N, P and Si) consumption and organic matter production in a coastal inlet affected by upwelling. Mar. Chem. 69, 217–236.

Pérez, F.F., Padín, X.A., Pazos, Y., Gilcoto, M., Cabanas, M., Pardo, P.C., Doval, M.D., Farina-Busto, L., 2010. Plankton response to weakening of the Iberian coastal upwelling. Global Change Biol. 16, 1258–1267.

Pérez-Camacho, A., Labarta, U., Beiras, R., 1995. Growth of mussels (*Mytilus edulis galloprovincialis*) on cultivation rafts: influence of seed source, cultivation site and phytoplankton availability. Aquaculture 138, 349–362.

Piedracoba, S., Álvarez–Salgado, X.A., Rosón, G., Herrera, J.L., 2005a. Short-timescale thermohaline variability and residual circulation in the central segment of the coastal upwelling system of the Ría de Vigo (northwest Spain) during four contrasting periods. J. Geophys. Res. 110, doi:10.1029/2004JC002556.

Piedracoba, S., Souto, C., Gilcoto, M., Pardo, P.C. 2005b. Hydrography and dynamics of the Ría de Ribadeo (NW Spain), a wave driven estuary. Estuar. Coast. Shelf Sci. 65, 726–738.

Plew, D.R., Stevens, C.L., Spigel, R.H., Hartstein, N.D. 2005. Hydrodynamic implications of large offshore mussel farms. IEEE J. Oceanic Eng. 30, 95–108.

Plew DR 2011 Shellfish farm-induced changes to tidal circulation in an embayment, and implications for seston depletion. Aquacult Environ Interact 1, 201–214

Prego, R., Barciela, M.C., Varela, M., 1999. Nutrient dynamics in the Galician coastal area (North western Iberian Peninsula): do the Rias Bajas receive more nutrient salts than the Rias Altas? Cont. Shelf Res. 19, 317–334.

Sánchez-Mata, A., Glémarec, M., Mora, J., 1999. Physico-chemical structure of the benthic environment of a Galician ría (Ría de Ares–Betanzos, north-west Spain). J. Mar. Biol. Assoc. UK 79, 1–21.

Stevens, C., Plew, D., Hartstein, N., Fredriksson, D. 2008. The physics of open-water shellfish aquaculture. Aquacult. Eng. 38, 145–160.

Strahler, A.N., 1963. Physical Geography. John Wiley and Sons, New York, 534pp.

Strohmeier, T., Aure, J., Duinker, A., Castberg, T., Svardal, A., Strand, O. 2005. Flow reduction, seston depletion, meat content and distribution of diarrhetic shellfish toxins in a long-line blue mussel (*Mytilus edulis*) farm. J. Shellfish Res. 24:15–23.

Tenore, K.R., Bouer, L.F., Cal, R.M., García-Fernández, C., González, N., González-Gurriaran, E., Hanson, R.B., Iglesias, J., From, M., López–Jamar, E., McClain, J., Pamatmat, M.M., Pérez, A., Rhoads, D.C., Santiago, G.D., Tietjen, J., Westrich, J., Windom, H.L., 1982. Coastal upwelling in the Rías Bajas, NW Spain: contrasting the benthic regimes in the Rías of Arosa and Muros. J. Mar. Res. 40, 701–770.

van Haren, H., 2001. Estimates of sea level, waves and winds from a bottom-mounted ADCP in a shelf sea. J. Sea Res. 45, 1–14.

Villegas-Ríos, D., Álvarez-Salgado, X.A., Piedracoba, S., Rosón, G., Labarta, U., Fernández-Reiriz, M.J., 2011. Net ecosystem metabolism of a coastal embayment fertilized by upwelling and continental runoff. Cont. Shelf Res. 31, 400–413.

Wing, S.R., Botsford, L.W., Ralston, S.V., Largier, J.L., 1998. Meroplanktonic distribution and circulation in a coastal retention zone of the northern California upwelling system. Limnol. Oceanogr. 43, 1710–1721.

Wooster, W.S., Bakun, A., McLain, D.R., 1976. Seasonal upwelling cycle along eastern boundary of North Atlantic. J. Mar. Res. 34, 131–141.

Figure captions:

Figure 1. Map of the Ría de Ares-Betanzos, showing the location where the acoustic 2D-ACM current meters were hung (black triangle) at Miranda, Lorbé, Redes and Arnela and the DCM12 mooring site in the middle ría (open triangle), the position where shelf winds were recorded by the buoy of Puertos del Estado at Cape Vilano (open dot), and the 4 km x 4 km cells where the Galician meteorological agency MeteoGalicia reconstructed the local winds (black circles). The inset shows the Lorbé and Arnela raft polygons.

Figure 2. Tidal height derived from the high precision quartz pressure sensor of the DCM12 current meter (a), East (black) and North (grey) total current velocity components for the four 2D-ACM current meters hung at 1 m depth at the bow of the rafts of Arnela (b), Lorbé (c), Miranda(d) and Redes (e) and for the five layers (f, g, h, i, j) Central, D1-D5 of the DCM12 Doppler current meter.

Figure 3. Counter-clockwise (blue) and clockwise components of the Fourier transform of current velocities for the four 2D-ACM current meters hung at 1m depth at the bow of the four rafts (A - Arnela, L- Lorbé, M - Miranda and R – Redes). Frequency is in day^{-1} (d^{-1}).

Figure 4. Counter-clockwise (blue) and clockwise components of the Fourier transform of current velocities for the five layers (up to down, D1-D5) of the DCM12 Doppler current meter moored mid-channel. Frequency is in day^{-1} (d^{-1}). Notice the vertical maximum at semidiurnal tidal frequencies in all layers, especially layer 2. Incidentally, the maximum in layer 1 occurs at 1 d^{-1} not $2d^{-1}$.

Figure 5. East (black) and North (grey) subtidal wind velocity components obtained from the Seawatch buoy of the Spanish Agency Puertos del Estado off

Cape Vilano (a), East (black) and North (grey) subtidal current velocity components for the four 2D-ACM current meters hung at 1m depth at the bow of the rafts of (b) Arnela, (c) Lorbé, (d) Miranda and (e) Redes and for the five layers (f, g, h, i, j) Central, D1-D5 of the DCM12 Doppler current meter. Note that Figure 5a shows the direction in which the wind is blowing to.

Figure 6. Progressive vector diagram for the low-pass filtered currents derived from 2D-ACM current meters hung at 1 m depth at the bow of the four rafts (A, L, R and M) and for the low-pass filtered currents derived from the first layer of the DCM12 (D) for the period 15 October 2007 to 20 November 2007. The origin (15 October 2007) is denoted with an asterisk and A, L, R, M and D for each current meter. Each dot from the asterisk indicates a day from 16 October to 20 November. The scale was multiplied by 10^{-1} km to facilitate the visualization of the trajectories.

Figure 7. Cross correlation coefficients (r) and phases (pha) between the residual surface current in the middle Ría de Ares-Betanzos (D1) and the subtidal current measured at 1 m depth at the bow of the four rafts (A1, L1, R1 and M1) as a function of the lag time (in hours) between residual currents for the time period 15 October-20 November 2007.

Figure 8. Cross correlation coefficients (r) and phases (pha) between the residual currents measured at 1 m depth at the bow of the four rafts (A1, L1, R1 and M1) as a function of the lag time (hours) between residual currents for the time period 15 October-20 November 2007.

Figure 1

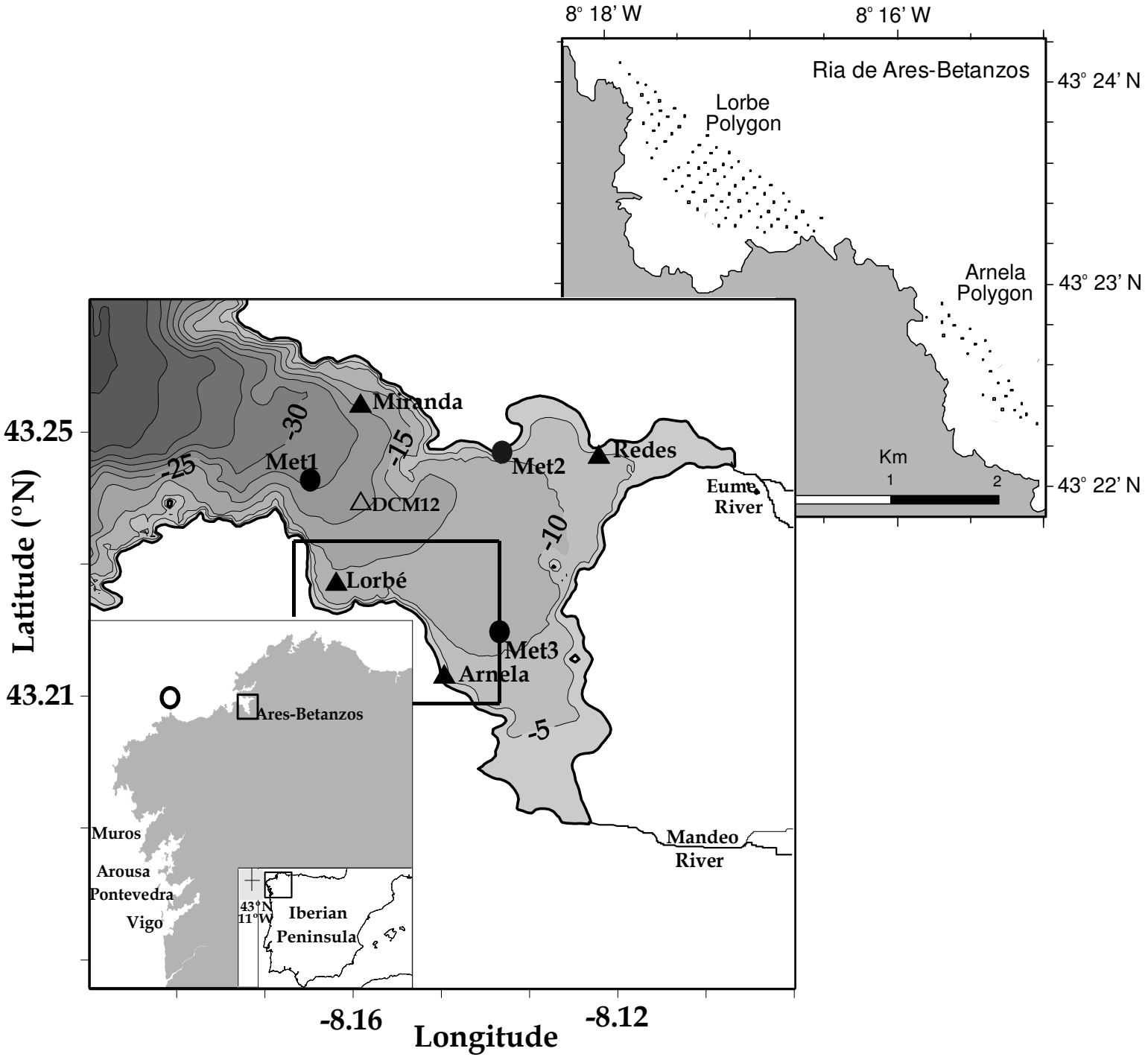
8° 18' W
8° 16' W
Ria de Ares-Betanzos
43° 24' N
43° 23' N
43° 22' N
Lorbe
Polygon
Arnela
Polygon
Km
1
2
Miranda
Met1
Met2
Redes
DCM12
Eume
River
Lorbé
Met3
Arnela
Ares-Betanzos
Muros
Arousa
Pontevedra
Vigo
43°N
11°W
Iberian
Peninsula
Mandeo
River
-30
-25
-15
-10
-5
0
43.25
43.21
Latitude (°N)
-8.16
-8.12
Longitude

Figure 2

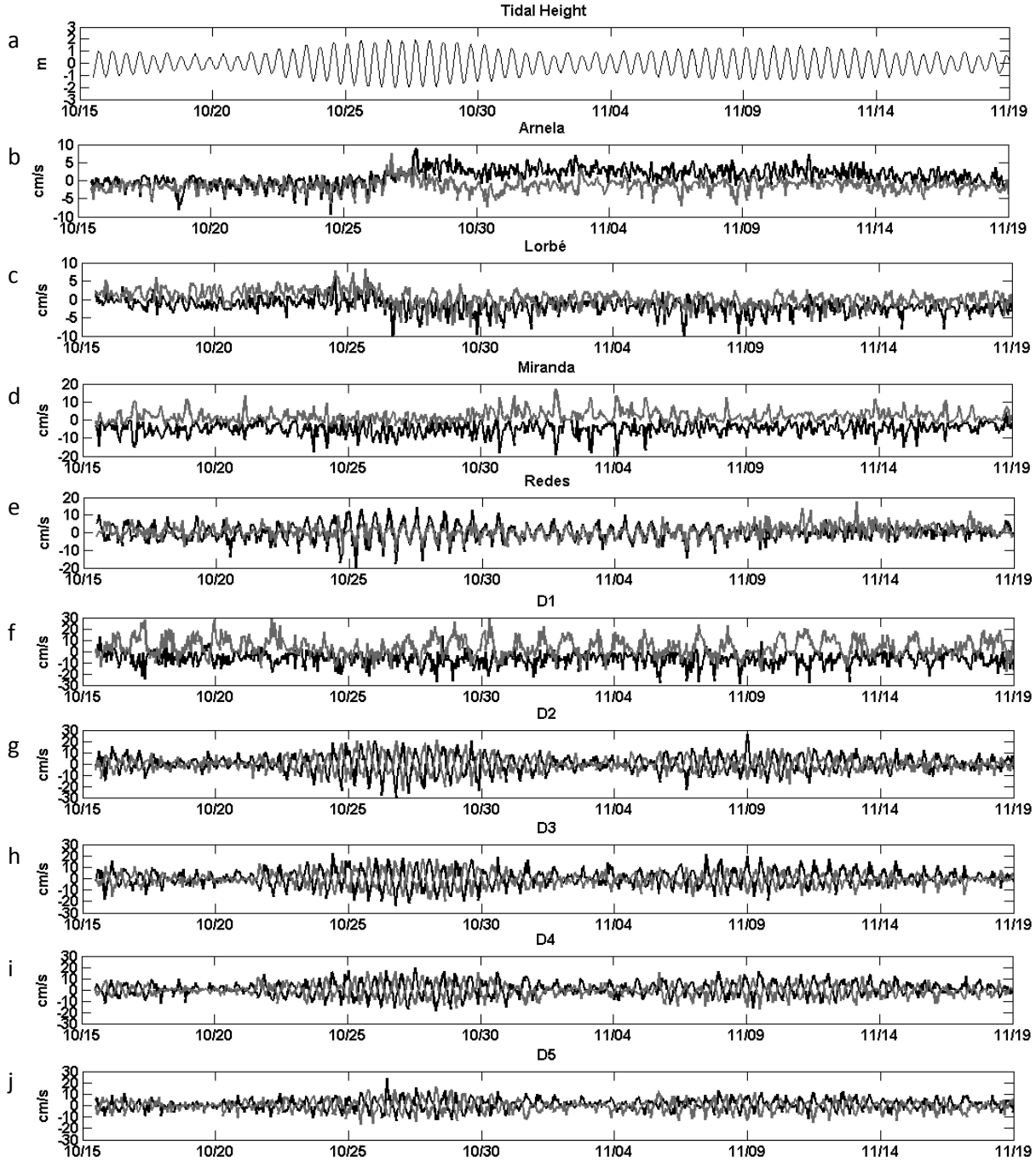
a
Tidal Height
m
b
Arnela
cm/s
c
Lorbé
cm/s
d
Miranda
cm/s
e
Redes
cm/s
f
D1
cm/s
g
D2
cm/s
h
D3
cm/s
i
D4
cm/s
j
D5
cm/s
10/15
10/20
10/25
10/30
11/04
11/09
11/14
11/19

Figure 3

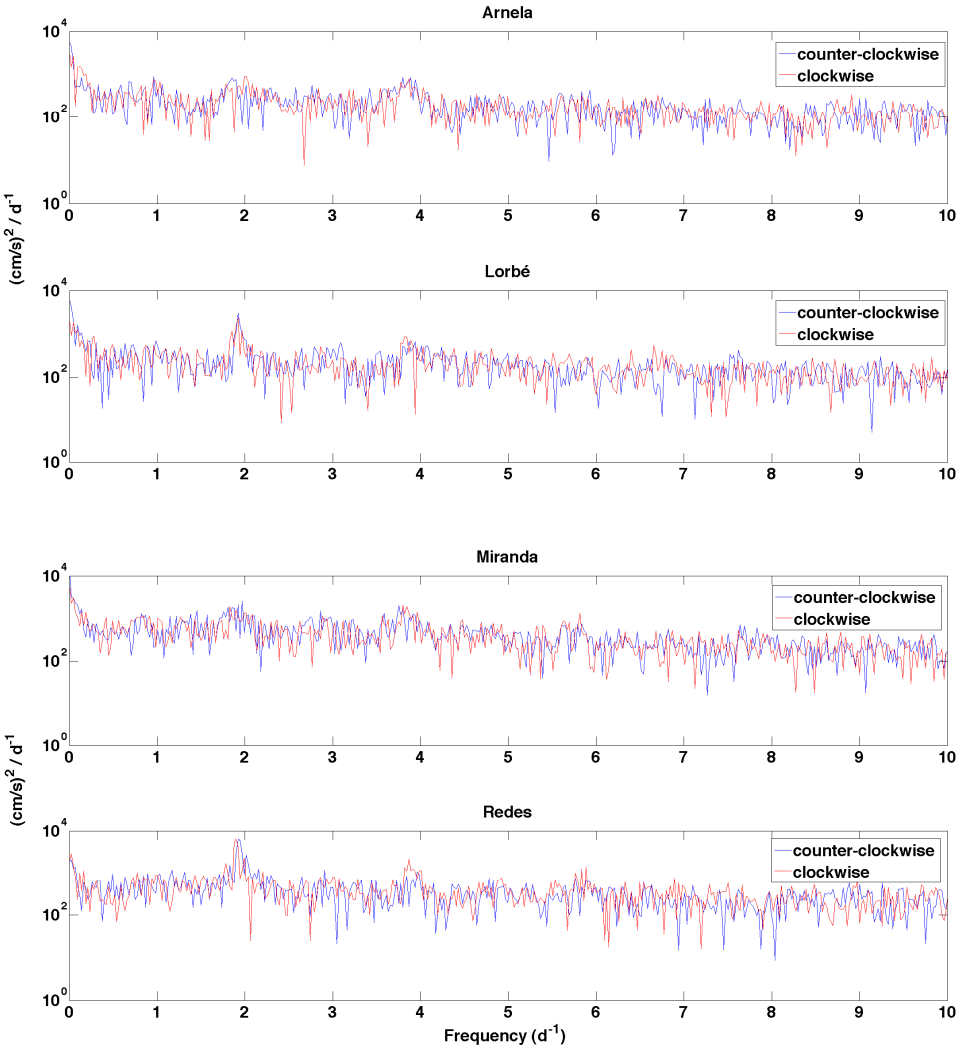
Arnela
Lorbé
Miranda
Redes
counter-clockwise
clockwise
(cm/s)^2 / d^{-1}
Frequency (d^{-1})

Figure 4

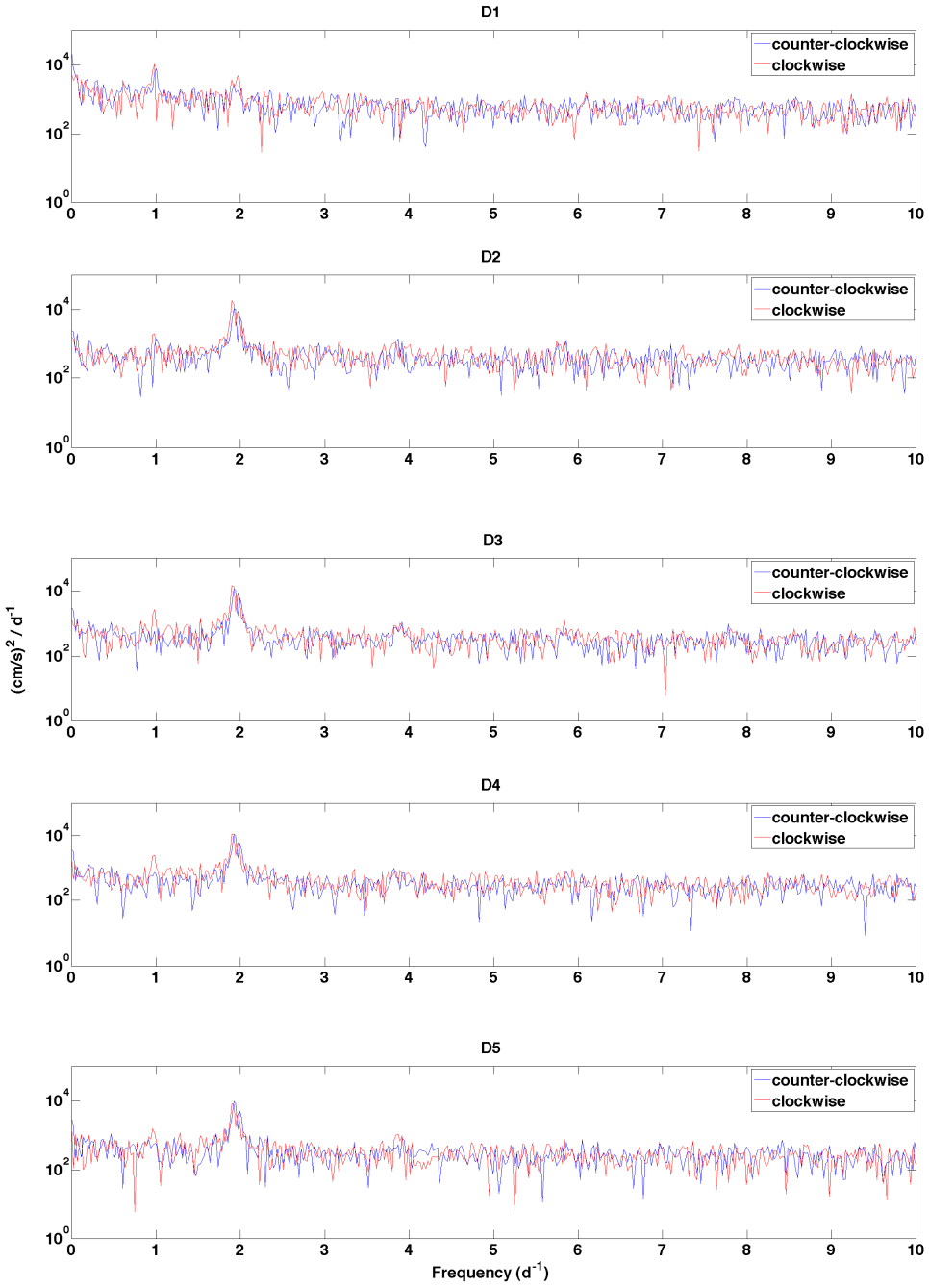
D1
D2
D3
D4
D5
counter-clockwise
clockwise
(cm/s)^2 / d^{-1}
Frequency (d^{-1})

Figure 5

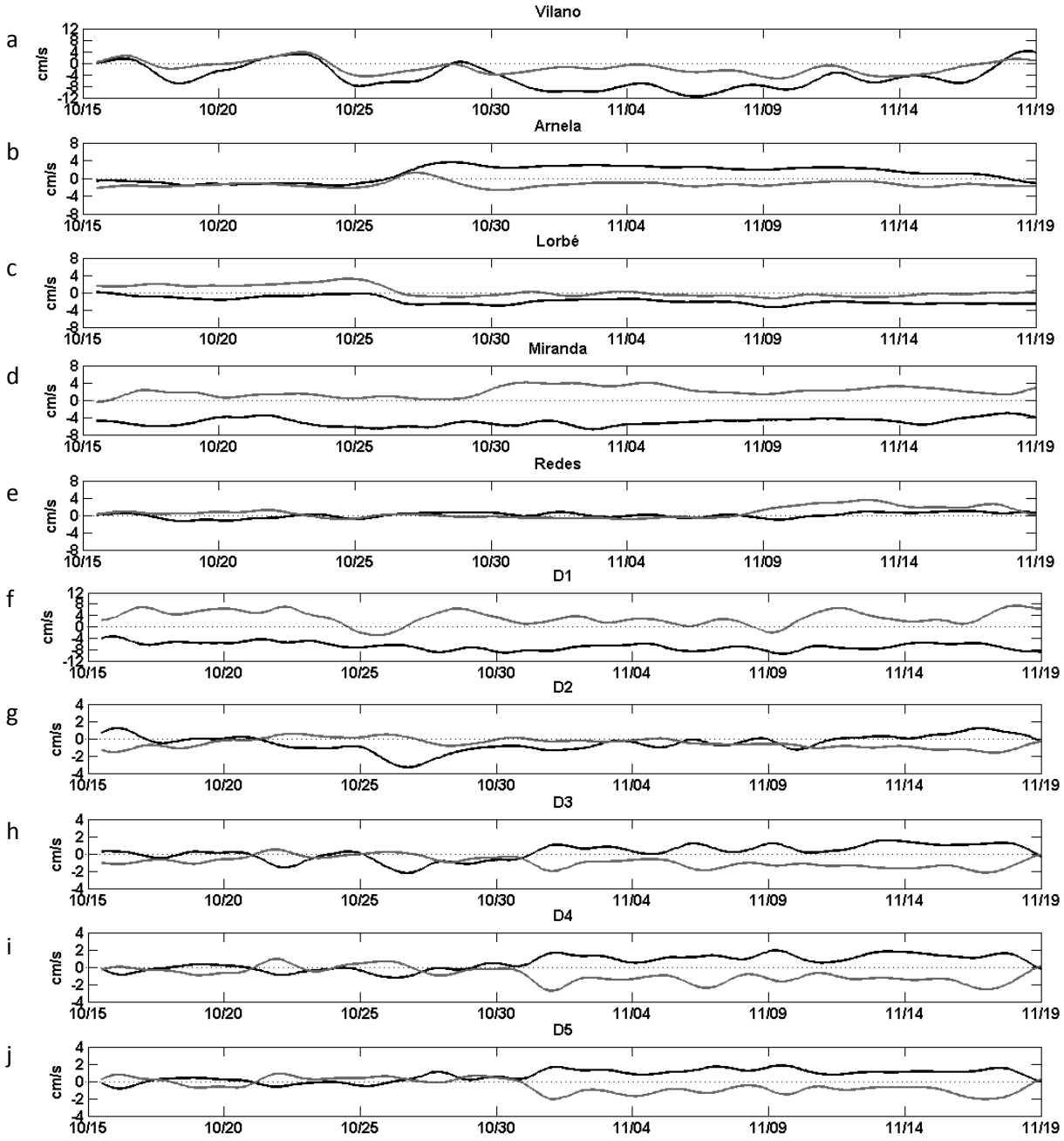
a
Vilano
b
Arnela
c
Lorbé
d
Miranda
e
Redes
f
D1
g
D2
h
D3
i
D4
j
D5
cm/s
10/15
10/20
10/25
10/30
11/04
11/09
11/14
11/19

Figure 6

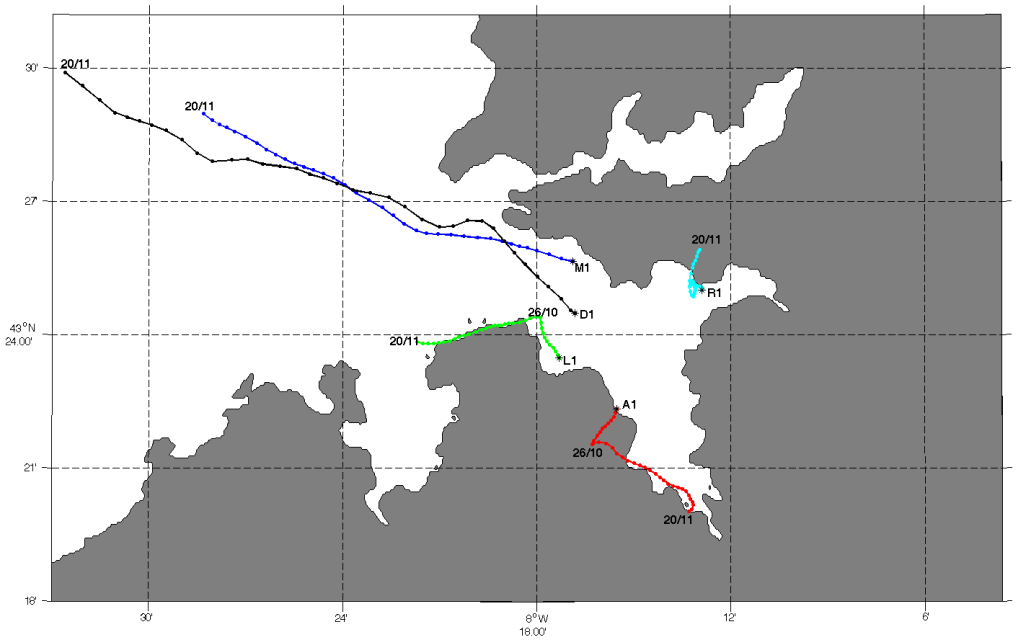
30'
27'
43°N
24.00'
21'
18'
30'
24'
8°W
18.00'
12'
6'
20/11
20/11
M1
20/11
R1
26/10
D1
20/11
L1
A1
26/10
20/11

Figure 7

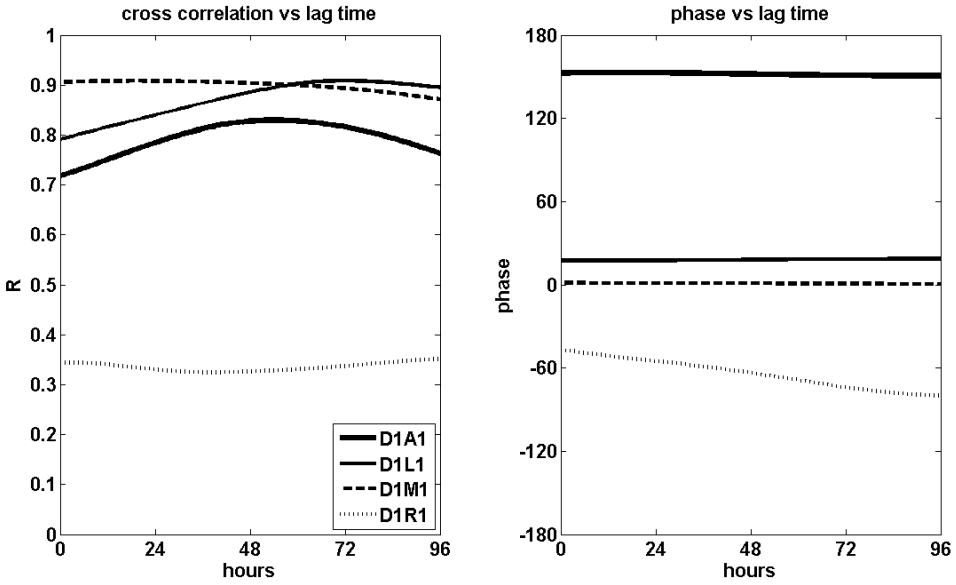
cross correlation vs lag time
R
hours
D1A1
D1L1
D1M1
D1R1
phase vs lag time
phase
hours

Figure 8

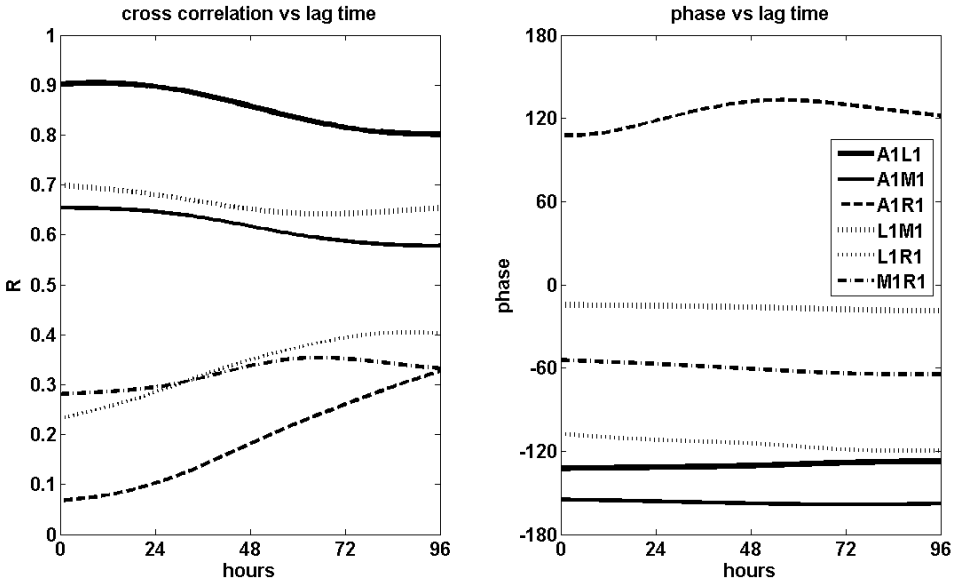
cross correlation vs lag time
R
hours
0
24
48
72
96
0.1
0.2
0.3
0.4
0.5
0.6
0.7
0.8
0.9
1
phase vs lag time
phase
180
120
60
0
-60
-120
-180
A1L1
A1M1
A1R1
L1M1
L1R1
M1R1

Table 1

constituent	major (cm/s)	emaj	minor (cm/s)	emin	inc (deg)	einc	pha (deg)	epha	snr
			Arnela 1						
***MSF**	0.1	0.1	-0.1	0.1	11	60	82	50	2.0
***ALP1**	0.2	0.1	-0.1	0.2	180	47	20	39	4.5
***2Q1**	0.2	0.1	0.2	0.1	30	49	253	40	2.6
***NO1**	0.2	0.1	0.2	0.1	9	122	172	117	3.4
***K1**	0.3	0.2	-0.2	0.1	65	24	49	33	3.5
***OO1**	0.1	0.2	0.1	0.1	11	67	339	52	2.1
***N2**	0.3	0.2	0.2	0.2	54	92	121	95	2.9
***S2**	0.4	0.3	-0.2	0.2	86	34	21	45	2.0
***ETA2**	0.2	0.1	-0.2	0.1	94	69	188	83	2.8
			Lorbé 1						
***Q1**	0.3	0.1	-0.2	0.2	69	33	23	31	5
***NO1**	0.3	0.1	0.2	0.2	30	36	298	30	3
***K1**	0.3	0.1	0.2	0.1	25	34	58	33	4
***UPS1**	0.2	0.2	-0.1	0.2	64	39	161	35	4
***MU2**	0.5	0.2	-0.1	0.3	89	27	66	28	4
***N2**	0.6	0.2	0.2	0.2	113	24	76	26	7
***M2**	1.7	0.2	0.1	0.3	139	8	150	8	57
***L2**	0.3	0.2	0.2	0.2	77	52	44	51	3
***S2**	0.7	0.2	-0.1	0.3	138	19	164	20	9
***MK3**	0.2	0.1	0.2	0.1	41	52	209	50	3
***MN4**	0.3	0.2	-0.2	0.2	27	48	35	37	4
***M4**	0.5	0.2	-0.2	0.2	29	22	116	20	9
***MS4**	0.4	0.2	-0.1	0.2	14	29	139	26	5
***S4**	0.3	0.2	0.1	0.2	46	42	135	47	2
***M8**	0.2	0.1	0.1	0.1	34	46	143	47	2
			Miranda 1						
***ALP1**	0.6	0.4	0.2	0.4	148	48	292	52	2
***2Q1**	0.6	0.4	0.1	0.4	135	44	28	52	3
***MU2**	1.3	0.9	0.2	0.8	140	38	334	44	2
***M2**	1.0	0.7	-0.1	0.9	108	77	189	41	2
			Redes 1						
***MSF**	0.2	0.1	0.1	0.1	48	44	66	39	2
***2Q1**	0.3	0.2	-0.1	0.3	1	67	182	47	3
***Q1**	0.4	0.2	0.2	0.3	36	53	116	46	3
***K1**	0.4	0.3	-0.1	0.4	164	57	206	41	2
***EPS2**	1.0	0.5	0.2	0.5	21	33	26	28	4
***N2**	2.7	0.6	-0.7	0.6	21	13	337	12	24
***M2**	4.2	0.5	0.3	0.5	21	8	355	8	70
***L2**	1.4	0.5	0.6	0.5	20	30	172	25	9
***S2**	1.4	0.4	0.1	0.5	22	23	319	22	10
***ETA2**	0.5	0.3	0.2	0.3	26	58	87	49	3
***MO3**	0.3	0.2	-0.1	0.2	148	37	100	38	3
***M3**	0.5	0.2	0.1	0.2	27	28	227	35	4
***SN4**	0.7	0.5	-0.4	0.2	89	30	165	60	2

Table 1. Parameters of the harmonic tidal analysis at the raft positions for the period from 15 October to 20 November 2007. Only constituents with signal-to-noise ratio >2 are listed. Percents of total variance explained were 16.8%, 53.4%, 14.3% and 64.1% for Arnela 1 m, Lorbé 1 m, Miranda 1 m and Redes 1 m, respectively.

Table 2

constituent	major (cm/s)	emaj	minor (cm/s)	emin	inc (deg)	einc	pha (deg)	epha	snr
			LAYER 1						
***2Q1**	0.9	0.6	0.5	0.7	2	121	37	65	2
***O1**	1.3	0.9	-0.1	0.7	121	29	17	47	2
***NO1**	1.1	0.6	0.1	0.7	39	41	218	36	3
***K1**	5.4	1.1	-0.8	0.5	91	6	248	14	24
***N2**	1.0	0.6	-0.2	0.6	128	47	124	47	2
***M2**	2.2	0.8	-0.4	0.7	132	21	68	17	8
***L2**	1.2	0.7	-0.3	0.8	4	41	193	33	3
***S2**	2.1	0.7	-0.8	0.6	143	25	104	23	10
			LAYER 2						
***K1**	1.1	0.2	-0.2	0.2	143	14	16	14	18
***J1**	0.4	0.2	-0.1	0.2	2	31	256	39	3
***OO1**	0.2	0.1	0.1	0.1	81	61	189	55	2
***MU2**	1.2	0.6	-0.2	0.7	134	28	64	34	4
***N2**	3.1	0.6	-0.4	0.7	134	12	132	11	27
***M2**	10.7	0.8	-2.4	0.7	143	4	78	4	190
***L2**	0.9	0.6	-0.2	0.7	106	50	180	47	2
***S2**	5.2	0.7	-0.9	0.6	144	7	100	8	57
***M4**	0.7	0.3	0.2	0.4	115	33	196	31	4
***2MN6**	0.4	0.2	-0.2	0.2	147	34	284	41	3
***M6**	0.3	0.2	-0.2	0.2	147	78	261	84	2
***2MS6**	0.4	0.2	0.1	0.2	158	31	249	31	4
			LAYER 3						
***2Q1**	0.5	0.2	-0.2	0.2	141	23	15	24	5
***Q1**	0.3	0.2	-0.1	0.2	44	35	320	40	3
***O1**	0.2	0.2	-0.2	0.2	99	67	60	40	2
***NO1**	0.3	0.2	-0.2	0.2	153	33	262	45	2
***K1**	0.9	0.2	-0.7	0.2	152	44	313	49	19
***J1**	0.4	0.2	-0.1	0.2	121	38	335	30	6
***MU2**	1.1	0.5	-0.2	0.4	135	26	44	26	5
***N2**	2.5	0.5	-0.2	0.5	138	10	134	10	28
***M2**	10.2	0.5	-1.2	0.4	144	3	81	2	410
***S2**	4.9	0.4	-0.7	0.5	143	5	98	5	130
***MN4**	0.4	0.2	0.1	0.3	135	38	274	39	4
***M4**	0.5	0.3	-0.2	0.2	150	30	247	48	2
***SN4**	0.4	0.2	0.1	0.3	102	64	220	46	4
***MS4**	0.5	0.3	-0.2	0.3	138	32	244	36	3
***M6**	0.3	0.2	-0.1	0.2	141	31	273	36	3
***2MS6**	0.4	0.2	-0.1	0.2	144	32	255	32	4
***M8**	0.1	0.2	-0.1	0.2	160	39	322	38	2

			LAYER 4						
***O1**	0.3	0.1	-0.1	0.2	85	99	105	43	3
***NO1**	0.5	0.3	-0.2	0.2	149	28	216	35	4
***K1**	0.9	0.3	-0.6	0.2	30	41	63	49	9
***J1**	0.4	0.2	-0.2	0.2	130	61	332	68	3
***MU2**	1.2	0.4	0.1	0.5	136	25	38	22	9
***N2**	2.0	0.5	0.1	0.5	138	14	132	13	14
***M2**	8.6	0.5	-0.1	0.5	141	3	77	3	300
***S2**	4.1	0.4	-0.2	0.5	137	7	95	6	93
***MN4**	0.4	0.3	0.1	0.3	100	52	273	40	3
***M4**	0.4	0.3	-0.1	0.3	126	54	235	57	2
***MS4**	0.5	0.3	-0.1	0.3	136	42	238	39	2
***2MS6**	0.3	0.2	-0.1	0.2	118	41	261	42	3
			LAYER 5						
***O1**	0.4	0.2	-0.2	0.2	143	28	81	34	5
***NO1**	0.5	0.2	-0.1	0.2	167	21	227	26	7
***K1**	0.5	0.2	-0.3	0.2	53	32	40	29	9
***MU2**	0.8	0.4	0.2	0.4	129	33	26	36	3
***N2**	1.7	0.4	0.3	0.4	137	14	127	14	19
***M2**	6.8	0.4	0.4	0.4	132	4	65	4	280
***S2**	3.2	0.5	0.2	0.4	130	7	82	7	49
***M4**	0.5	0.2	-0.1	0.3	126	38	222	40	5
***SN4**	0.4	0.2	-0.2	0.3	96	52	189	38	4
***MS4**	0.5	0.2	0.0	0.2	140	27	258	33	5
***2MS6**	0.3	0.2	-0.1	0.2	111	36	213	47	3

Table 2. Parameters of the harmonic tidal analysis for the five layers of the middle mooring for the period from 15 October to 20 November 2007. Only constituents with signal-to-noise ratio >2 are listed. Percents of total explained variance were 51.5%, 91.1%, 91.2%, 87.9% and 86.0% for layers 1, 2, 3, 4 and 5, respectively.

Table 3

lag time (H)	r WD1	r WD2	r WD3	r WD4	r WD5	pha WD1 (deg)	pha WD2 (deg)	pha WD3 (deg)	pha WD4 (deg)	pha WD5 (deg)
0-12	**0.78**	**0.56**	0.67	0.80	0.84	**-33.24**	**14.67**	88.62	105.17	119.31
13-24	0.77	0.56	0.67	0.79	0.86	-35.45	17.31	86.59	103.70	118.02
25-36	0.76	0.55	0.67	0.79	**0.86**	-38.44	20.42	84.43	102.58	**117.23**
37-48	0.76	0.54	0.67	0.80	0.86	-41.12	24.89	83.62	102.29	116.80
49-60	0.76	0.53	0.68	**0.80**	0.85	-42.79	30.75	84.34	**102.50**	116.58
61-72	0.77	0.53	0.70	0.80	0.81	-43.47	36.58	85.54	102.86	116.75
73-84	0.77	0.52	0.71	0.79	0.77	-43.62	40.71	86.47	103.40	117.44
85-96	0.78	0.51	**0.73**	0.79	0.74	-43.47	42.95	**87.62**	104.38	118.41

Table 3. Average cross correlation coefficients (r) and phases (pha) between the residual current measured in the five layers in the middle Ría de Ares-Betanzos (D1-D5) and the residual shelf winds recorded at the Cape Vilano buoy (W), as a function of the lag time (hours) between residual currents and winds for the time period 15 October-20 November 2007. The correlation coefficients were calculated for a discrete time. After this, we calculate the average correlation coefficient and phase over 12 hour intervals (0–12, 13–24, 25–36, … 85–96 hours). Two-tailed critical values of r for 23 degrees of freedom are 0.33, 0.40, 0.46 and 0.51 for $p = 0.1$, $p = 0.05$, $p = 0.02$ and $p = 0.01$ respectively.

Table 4

lag time (H)	r WA1	r WL1	r WM1	r WR1	pha WA1	pha WL1	pha WM1	pha WR1
0-12	0.69	0.74	**0.79**	0.20	123.94	-14.43	**-42.50**	-105.53
13-24	0.70	0.76	0.77	0.25	127.08	-12.01	-42.44	-112.96
25-36	0.72	0.79	0.75	0.31	129.31	-9.83	-42.34	-119.18
37-48	0.74	0.81	0.73	0.37	130.15	-8.11	-42.24	-122.70
49-60	**0.74**	**0.82**	0.72	0.40	**129.51**	**-7.50**	-42.36	-123.45
61-72	0.74	0.82	0.71	0.43	127.24	-7.59	-42.96	-123.10
73-84	0.73	0.81	0.71	0.44	123.80	-8.55	-43.96	-121.59
85-96	0.70	0.78	0.71	**0.45**	119.86	-10.23	-45.09	**-119.09**

Table 4. Average cross correlation coefficients (r) and phases (pha) between the residual current measured at 1m depth at the bow of the four rafts (A, L, R and M) and the residual shelf winds recorded at the Cape Vilano buoy (W), as a function of the lag time (hours) between residual currents and winds for the time period 15 October-20 November 2007. The correlation coefficients were calculated for a discrete time. After this, we calculate the average correlation coefficient and phase over 12 hour intervals (0–12, 13–24, 25–36, … 85–96 hours). Two-tailed critical values of r for 24 degrees of freedom are 0.32, 0.39, 0.45 and 0.50 for $p = 0.1$, $p = 0.05$, $p = 0.02$ and $p = 0.01$ respectively.